Supporting Information

Contrasting Effects of Organic Chloride Additives on Performance of Direct and Inverted Perovskite Solar Cells

Pang Wang[†,‡], Hui Wang[†,‡], Fanghao Ye[†,‡], Huijun Zhang[†,‡], Mengting Chen[†,‡], Jinlong Cai[†,‡], Donghui Li[†,‡], Dan Liu*[†,‡] and Tao Wang*[,†,‡]

[†] State Key Laboratory of Silicate Materials for Architectures, Wuhan University of Technology, Wuhan, 430070, China

[‡] School of Materials Science and Engineering, Wuhan University of Technology, Wuhan, 430070, China

*E-mail: dliu@whut.edu.cn; twang@whut.edu.cn

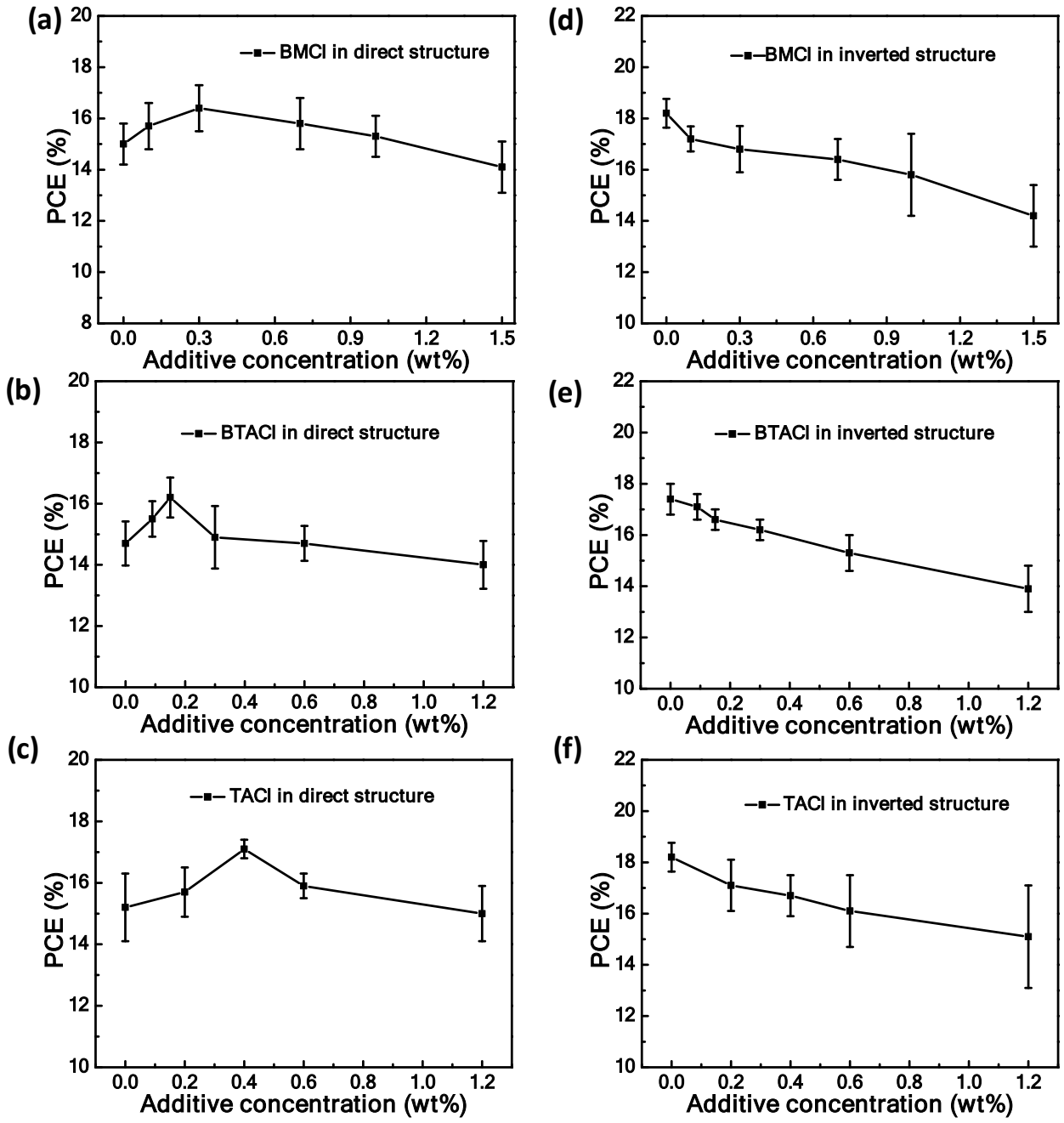

Figure S1. The PCE of PTAA-based devices as a function of additive content: (a, d) BMCl, (b, e) BTACl, (c, f) TACl. Panels (a-c) correspond to direct devices (ITO/TiO_2/$PC_{61}BM$/$MAPbI_3$/PTAA/MoO_3/Ag). Panels (d-f) correspond to inverted devices (ITO/PTAA/$MAPbI_3$/$PC_{61}BM$/ZrAcac/Ag).

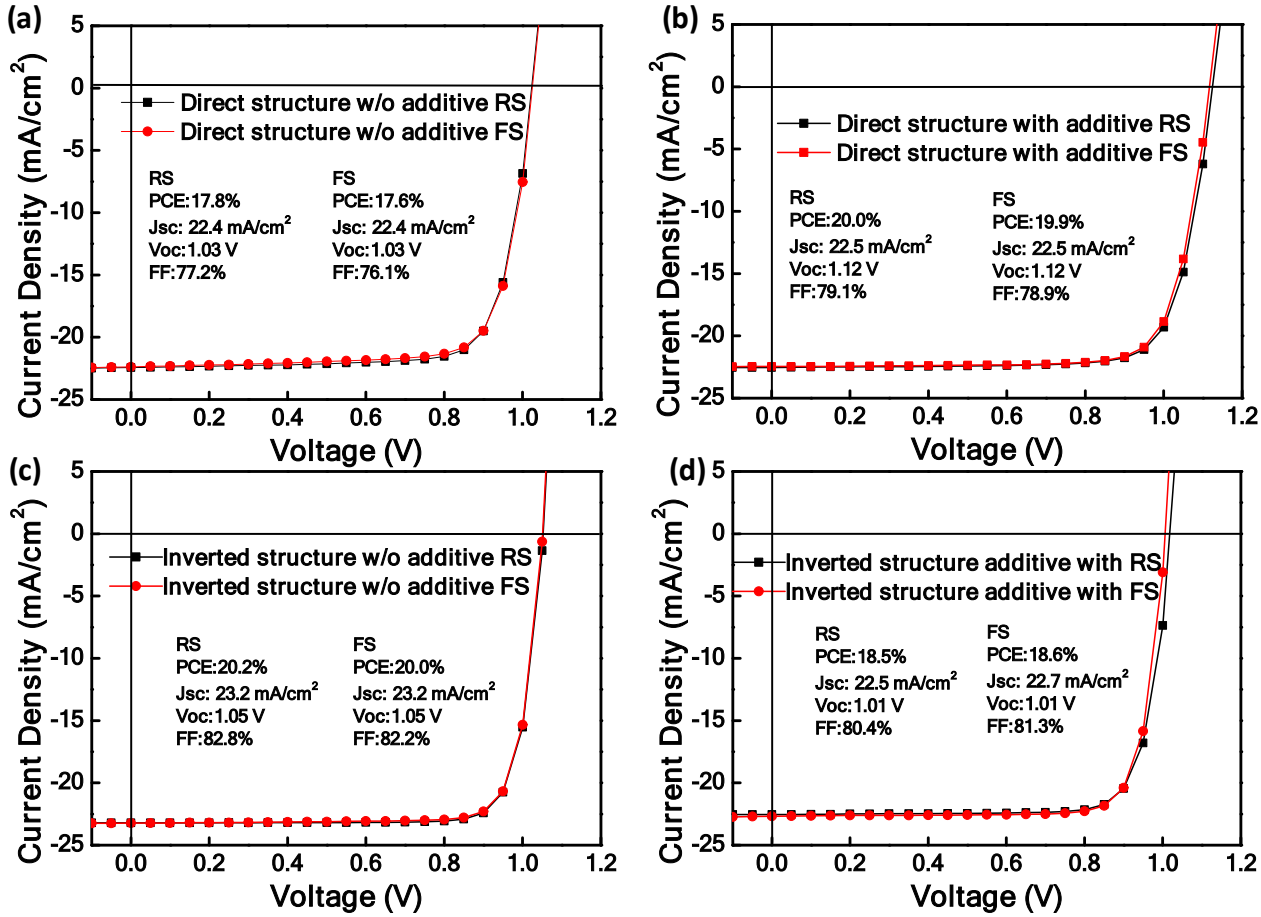

Figure S2. Best J-V curves from forward and reverse scans showing negligible hysteresis with the presence of an optimal amount of TACl additive, with polyTPD as the HTM. Direct devices (a) w/o and (b) with the presence of TACl. Inverted devices (c) w/o and (d) with the presence of TACl.

Table S1 Photovoltaic parameters of n-i-p and p-i-n type PSCs employing PTAA as the HTM.

Device type	Additive	Scanning Direction	V_{OC} (V)	J_{SC} (mA/cm^{-2})	FF (%)	PCE$_{ave}$* (PCE$_{max}$)
n-i-p	w/o	reverse	1.03±0.01	-22.0± 0.4	68.7±5.6	15.4±1.0(16.3)
		forward	1.03±0.01	-21.9± 0.4	67.5±5.1	15.2±1.1(16.1)
	BMCl	reverse	1.06±0.01	-21.7±0.4	72.1±3.3	16.5±0.6(17.5)
		forward	1.06±0.01	-21.5±0.6	71.9±4.3	16.4±0.5(17.1)
	BTACl	reverse	1.07±0.01	-21.9±0.3	69.1±2.8	16.3±0.6(17.0)
		forward	1.07±0.01	-21.9±0.3	68.0±2.6	16.2±0.7(16.8)
	TACl	reverse	1.05±0.01	-21.8±0.3	75.4±1.3	17.2±0.2(17.5)
		forward	1.05±0.01	-21.6±0.3	75.0±1.4	17.1±0.2(17.4)
p-i-n	w/o	reverse	1.03±0.01	-22.2± 0.2	79.7±2.0	18.2±0.6(19.1)
		forward	1.03±0.01	-22.2± 0.2	79.5±1.5	18.2±0.5(19.0)
	BMCl	reverse	1.01±0.01	-21.8±0.4	75.9±3.3	16.7±0.9(17.8)
		forward	1.01±0.01	-21.7±0.5	76.3±3.5	16.8±1.0(17.8)
	BTACl	reverse	0.99±0.01	-21.1±0.6	77.4±1.9	16.2±0.6(17.5)
		forward	0.99±0.01	-21.1±0.5	78.3±1.0	16.4±0.5(17.4)
	TACl	reverse	1.00±0.01	-21.3±0.7	76.9±3.8	16.3±1.2(17.8)
		forward	1.00±0.01	-21.2±0.8	77.4±3.0	16.4±1.3(17.9)

*The PCE$_{ave}$ ± error bar was obtained based on 20 individual devices.

Table S2 Photovoltaic parameters of n-i-p and p-i-n type PSCs employing PCDTBT8 as the HTM.

Device type	Additive	Scanning Direction	V_{OC} (V)	J_{SC} (mA/cm^{-2})	FF (%)	PCE$_{ave}$ (PCE$_{max}$)
n-i-p	w/o	reverse	1.00±0.01	-21.3±0.3	65.8±1.9	13.9±0.9(15.0)
		forward	1.00±0.02	-21.5±0.6	65.2±1.9	14.1±0.8(15.3)
	BMCl	reverse	1.02±0.01	-21.4±0.3	67.6±1.8	14.7±0.5(15.4)
		forward	1.02±0.01	-21.3±0.3	66.9±1.1	14.4±0.4(15.6)
	BTACl	reverse	1.02±0.01	-21.7±0.2	65.4±2.8	14.4±0.8(15.7)
		forward	1.02±0.01	-21.6±0.5	66.4±3.1	14.6±0.8(15.9)
	TACl	reverse	1.07±0.01	-21.1±0.6	69.5±4.0	15.7±0.3(16.3)
		forward	1.07±0.01	-21.1±0.6	69.4±4.1	15.6±0.6(16.6)
p-i-n	w/o	reverse	1.01±0.01	-21.5±0.3	73.7±3.8	16.0±0.6(16.8)
		forward	1.01±0.01	-21.7±0.2	75.5±1.7	16.4±0.4(16.9)
	BMCl	reverse	0.99±0.01	-19.7±0.4	70.5±2.5	13.7±0.9(15.1)
		forward	0.98±0.02	-19.9±0.4	65.4±3.6	12.8±0.8(14.0)
	BTACl	reverse	0.94±0.01	-20.2±0.4	69.4±3.1	13.2±0.8(14.4)
		forward	0.93±0.02	-20.5±0.5	67.7±3.6	12.8±0.7(13.7)
	TACl	reverse	0.98±0.01	-20.1±0.5	71.4±2.1	14.1±0.7(15.3)
		forward	0.98±0.02	-20.2±0.5	71.7±2.8	14.2±0.6(15.1)

* The error bars were obtained based on 20 individual devices.

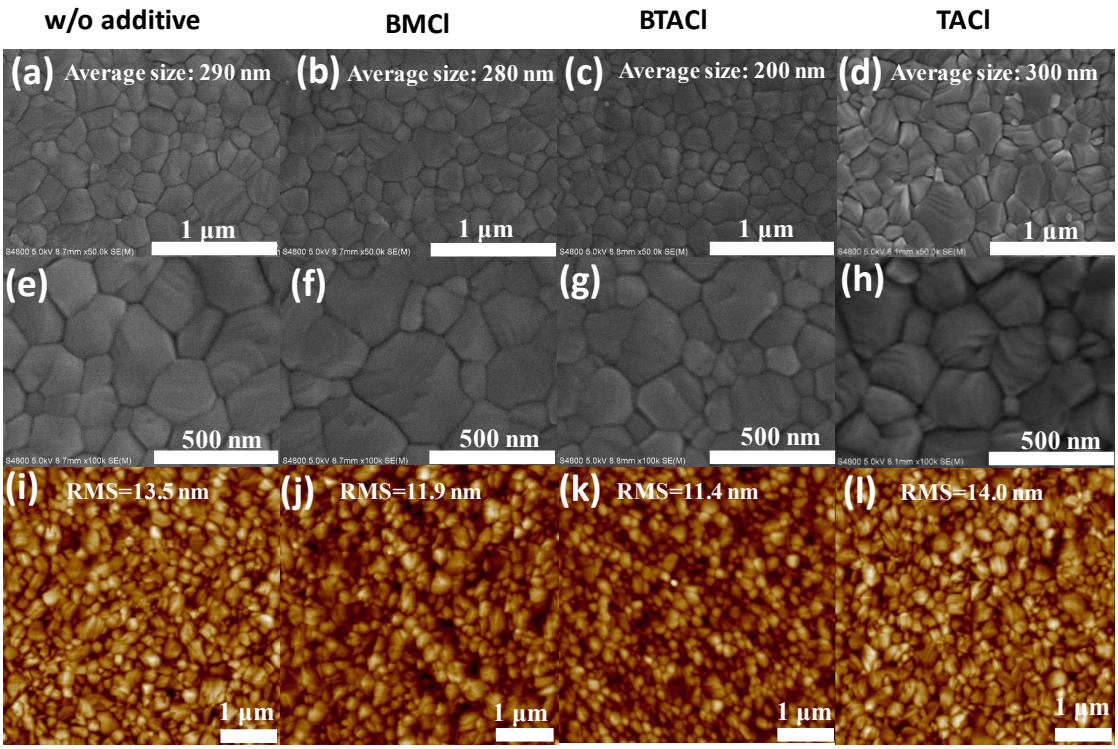

Figure S3 (a-h) SEM and (i-l) AFM topographic images of $MAPbI_3$ films. Panels (a, e, i) correspond to perovskite films without the presence of additives. Panels (b, f, j) correspond to perovskite film with the presence of BMCl. Panels (c, g, k) correspond to perovskite film with the presence of BTACl. Panels (d, h, l) correspond to perovskite film with the presence of TACl.

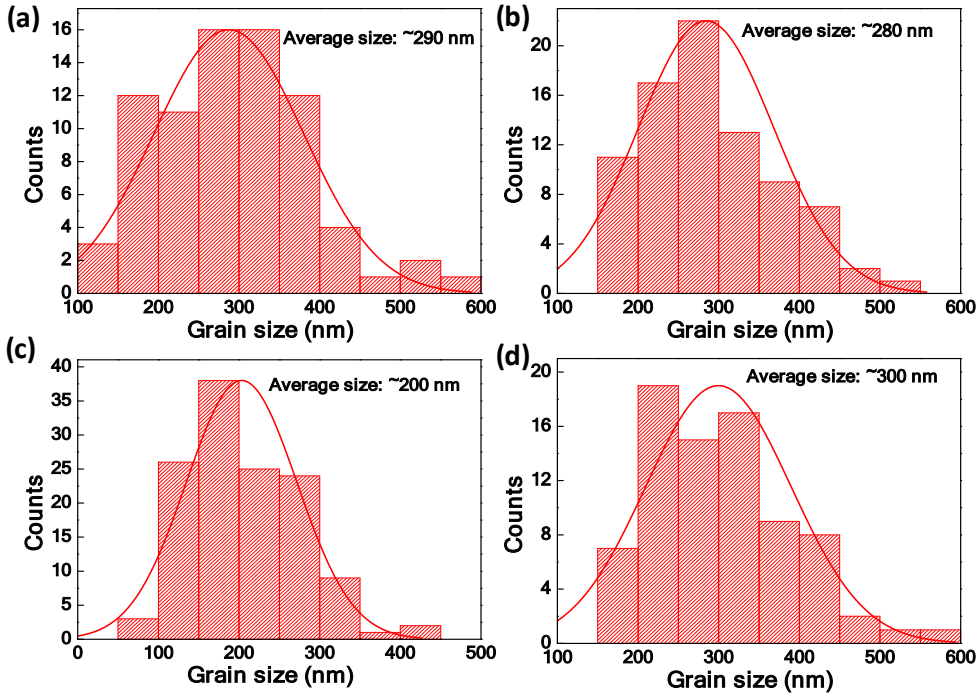

Figure S4. The statistical size distributions of perovskite grains analyzed from Figure 3. (a) w/o additive, and with the presence of an optimal amount of (b) BMCl, (c) BTACl and (d) TACl.

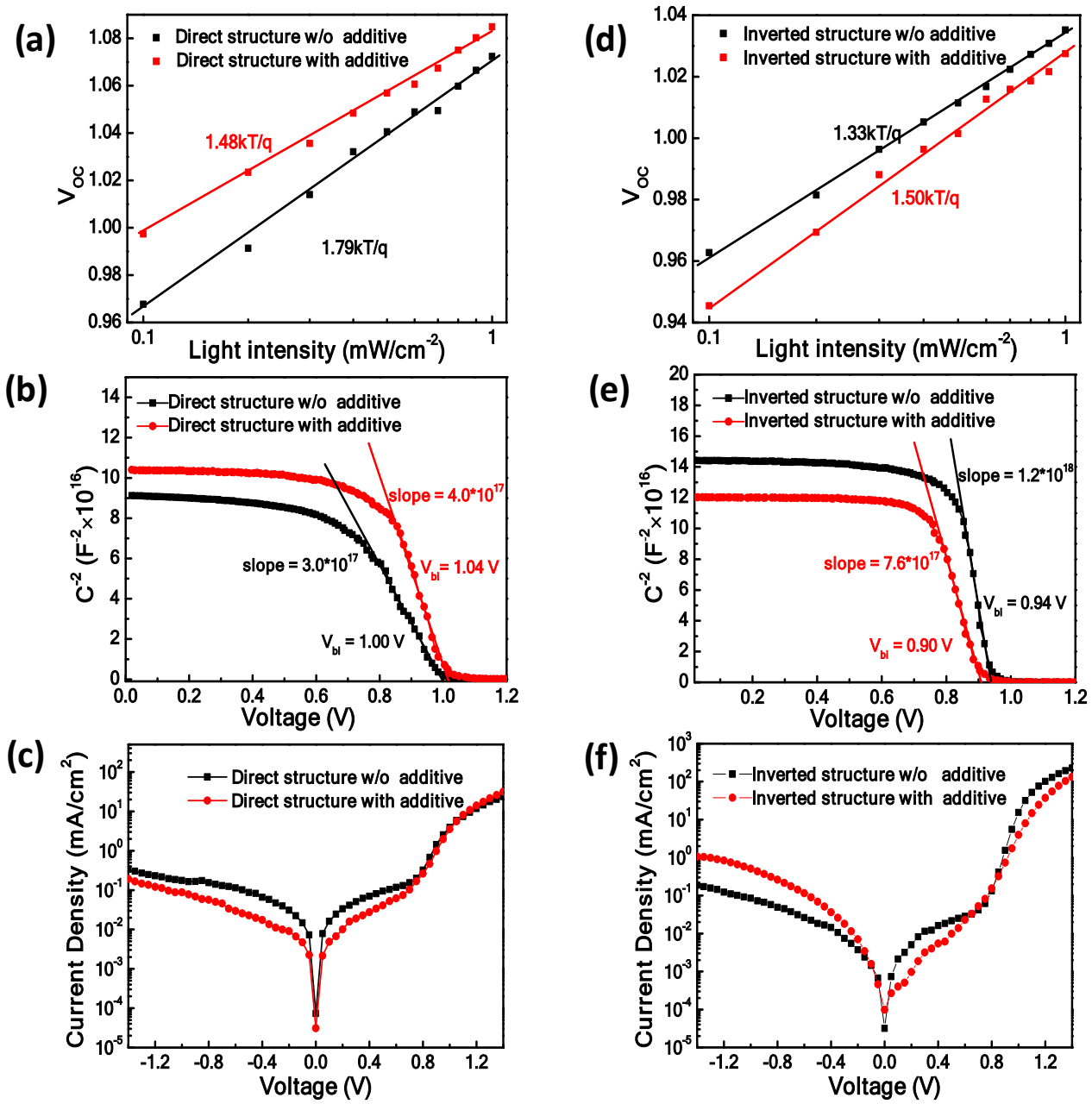

Fig. S5 (a, d) V_{OC} as a function of light intensity in a semi-log plot, (b, e) Mott−Schottky ($M-S$) plots at 10 kHz, (c, f) dark current density− voltage curve with and without TACl. Panels (a, b, c) correspond to direct structure devices, and panels (d, e, f) correspond to inverted structure devices.

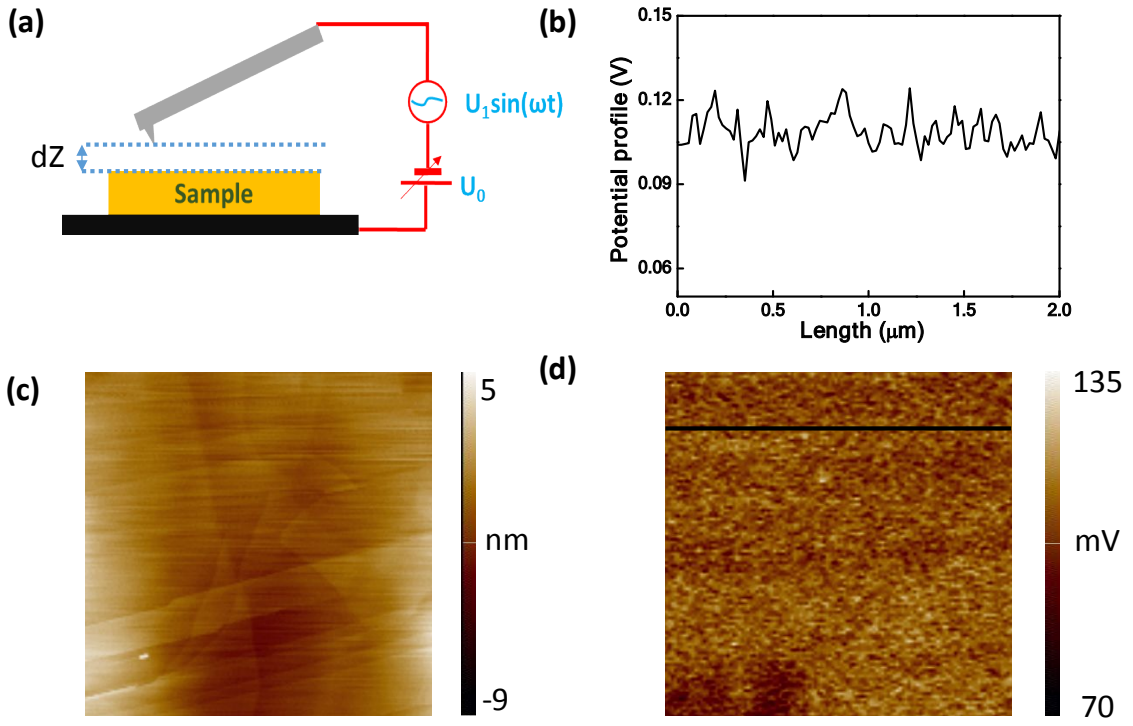

Figure S6. (a) Schematic diagram of the KPFM test. (b) Surface potential profile of HOPG. (c) Topographic and (d) Surface potential images of HOPG.

During the KPFM measurement, the surface topography of the sample (see Figure S4c,) was measured in the semi-contact mode in the first pass, then the probe was lifted to a height *dZ* during the second pass, using an alternating voltage $U_1 \cdot sin(\omega t)$ to control oscillations of the probe at corresponding resonance frequency and a direct bias U_0 to keep the oscillation amplitude of the probe at zero (Figure S4a). The surface electric potential can be acquired by recording U_0 across the whole sample when keeping the oscillation amplitude at zero and a constant distance *dZ*. The work function (WF) relation can be determined by the equation of $q \times \Delta V = \phi_{tip} - \phi_{sample}$, where q represents the element charge, ϕ_{tip} and ϕ_{sample} represent the WF of the probe and sample respectively.[1] Figure S4c and d show the topography and surface potential of highly oriented pyrolytic graphite (HOPG) respectively, and from the later an average surface potential of 109 mV can be determined (see Figure S4b). The WF of HOPG is 4.61 eV, and this marks ϕ_{tip} as 4.72 eV.

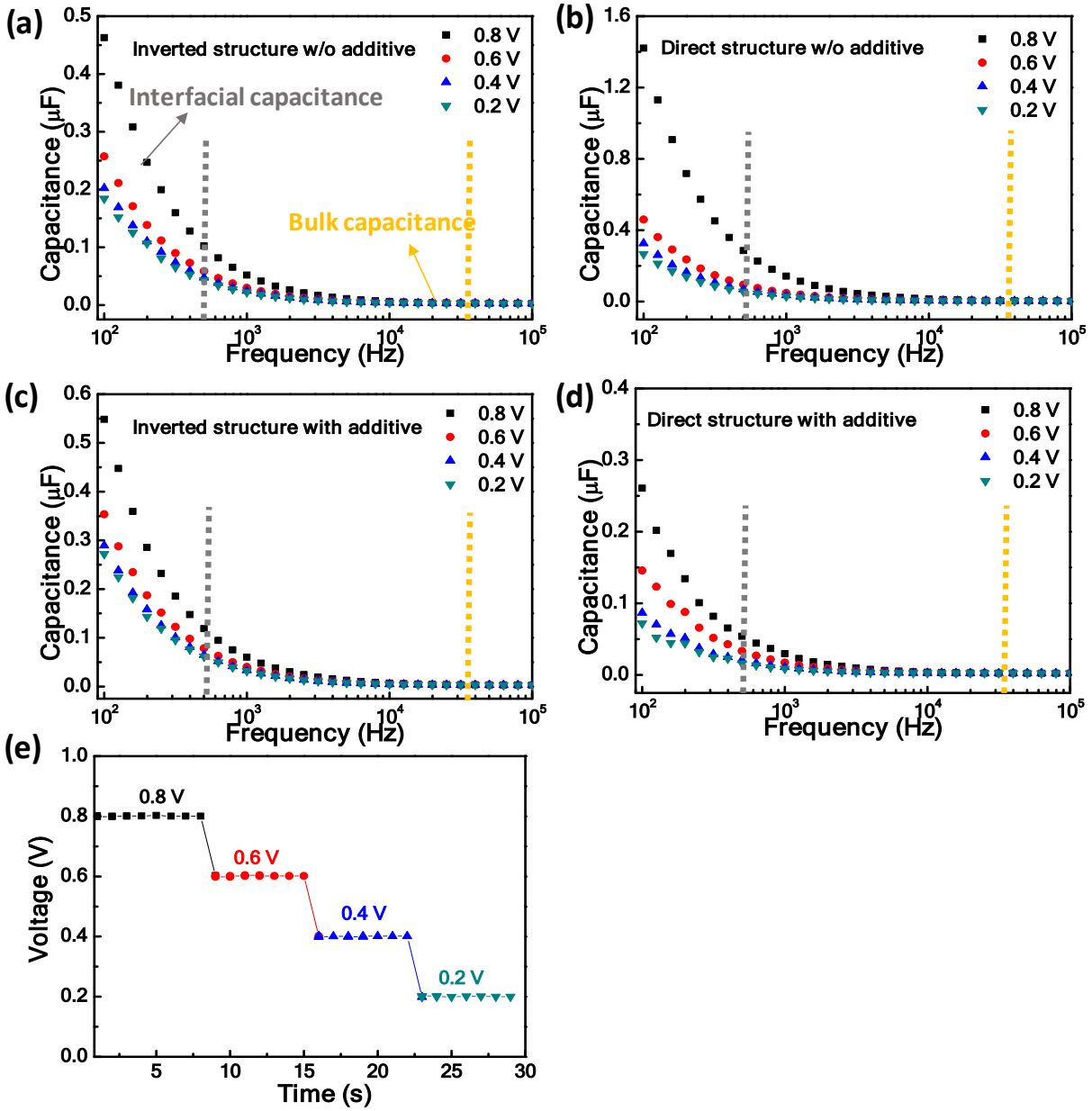

Figure S7. Capacitance-Frequency relation measured under 1 sun illumination from direct and inverted devices: (a) Inverted and (b) direct devices w/o TACl, (c) Inverted and (d) direct devices with TACl. (e) Voltage variations during the whole test process. The grey and yellow dashed lines represent the low frequency region (500 Hz) and high frequency region (12500 Hz), respectively.

Reference

[1] Y. Yan, F. Cai, L. Yang, W. Li, Y. Gong, J. Cai, S. Liu, R. S. Gurney, D. Liu, T. Wang, *ACS Appl. Mater. Interfaces* **2017**, *9*, 32678.